# Coherent dynamics of meta-toluidine investigated by quasielastic neutron scattering

Antonio Faraone, Kunlun Hong, Larry R. Kneller, Michael Ohl, and John R. D. Copley

Citation: The Journal of Chemical Physics **136**, 104502 (2012); doi: 10.1063/1.3691185
View online: http://dx.doi.org/10.1063/1.3691185
View Table of Contents: http://scitation.aip.org/content/aip/journal/jcp/136/10?ver=pdfcov
Published by the AIP Publishing

# Coherent dynamics of *meta*-toluidine investigated by quasielastic neutron scattering

Antonio Faraone,[1,2,a)] Kunlun Hong,[3] Larry R. Kneller,[1,2] Michael Ohl,[4] and John R. D. Copley[1]

[1]*NIST Center for Neutron Research, National Institute of Standards and Technology, Gaithersburg, Maryland 20899-6102, USA*
[2]*Department of Materials Science and Engineering, University of Maryland, College Park, Maryland 20742, USA*
[3]*Center for Nanophase Materials Sciences, Oak Ridge National Laboratory, Oak Ridge, Tennessee 37831, USA*
[4]*Jülich Center for Neutron Science at the Spallation Neutron Source, Oak Ridge National Laboratory, Oak Ridge, Tennessee 37831, USA*

(Received 11 October 2011; accepted 10 February 2012; published online 8 March 2012)

The coherent dynamics of a typical fragile glass former, *meta*-toluidine, was investigated at the molecular level using quasielastic neutron scattering, with time-of-flight and neutron spin echo spectrometers. It is well known that the static structure factor of *meta*-toluidine shows a prepeak originating from clustering of the molecules through hydrogen bonding between the amine groups. The dynamics of *meta*-toluidine was measured for several values of the wavevector transfer $Q$, which is equivalent to an inverse length scale, in a range encompassing the prepeak and the structure factor peak. Data were collected in the temperature range corresponding to the liquid and supercooled states, down to the glass transition. At least two dynamical processes were identified. This paper focuses on the slowest relaxation process in the system, the $\alpha$-relaxation, which was found to scale with the macroscopic shear viscosity at all the investigated $Q$ values. No evidence of "de Gennes" narrowing associated with the prepeak was observed, in contrast with what happens at the $Q$ value corresponding to the interparticle distance. Moreover, using partially deuterated samples, the dynamics of the clusters was found to be correlated to the single-particle dynamics of the *meta*-toluidine molecules. © *2012 American Institute of Physics*. [http://dx.doi.org/10.1063/1.3691185]

## I. INTRODUCTION

The slowing down of the dynamics of liquids well below their melting temperature, without the crystallization process taking place, down to a temperature where the microscopic relaxation happens on the experimental time scale, at the glass-transition, is one of the most interesting and still unresolved phenomenon. The dynamics of supercooled liquids and the glass transition, often characterized by strongly non-Arrhenius temperature dependence as well as markedly non-Debye relaxation processes, are still objects of intense debate in the scientific community. In the past twenty years, much effort has been devoted to the verification/falsification of one of the most successful theories for the description of the dynamics of supercooled liquids, the mode coupling theory (MCT).[1] More recently, triggered by both experimental and molecular dynamics simulation results, the role of dynamical heterogeneities has been highlighted.[2]

The metadisubstituted benzene, *meta*-toluidine (*m*-toluidine) with chemical formula $CH_3$-$C_6H_4$-$NH_2$ is a good glass former ($T_g$ = 183.5 K) with high fragility (fragility index $m$=79 ) (Refs. 3 and 4) in the classification scheme introduced by Angell.[4,5] Because of these characteristics it has been extensively studied in the past particularly for the validation of the MCT.[6,7] Another relevant characteristic of *m*-toluidine is the presence of molecular clusters, evidenced by a prepeak located at about 0.5 $Å^{-1}$, which are due to hydrogen bonding between the $NH_2$ groups. Morineau and Alba-Simionesco[8,9] investigated the properties of this feature as a function of both temperature and pressure using neutron scattering. Califano and co-workers investigated the clusters using computer simulations.[10,11] These groups agree that a limited number of molecules, usually estimated to be less than 10, because of the steric hindrance of the benzene rings, takes part in the clusters. Extensive dynamical measurements have been performed using both x rays[7] and light scattering[6], as well as mechanical relaxation methods[12,13] and dielectric spectroscopy.[14–16]

As already mentioned, neutron scattering has been used effectively to investigate the structure of *m*-toluidine.[8,9] However, as far as the relaxational dynamics is concerned, to the best of our knowledge, all that exists is a partially published work using coherent quasielastic neutron scattering (QENS) to investigate the dynamics of *m*-toluidine in the picoseconds to nanoseconds time scale.[17] This study highlighted that the dynamics of the system exhibit "de Gennes" narrowing, a slowing down of the dynamics, at a wavevector transfer $Q$ that corresponds to the molecules' center-to-center (CC) distance.[17] In fact, QENS allows the investigation of the relaxational dynamics over length scales ranging from fractions of an angstrom to tens of angstroms over time scales from picoseconds to tens of nanoseconds. In this respect, QENS is

a)Electronic mail: afaraone@nist.gov.

 

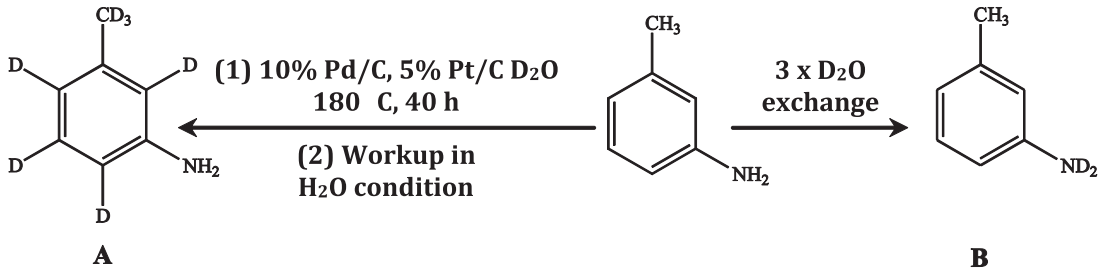


FIG. 1. Scheme describing the synthesis of the partially deuterated samples $C_7H_2D_7N$ (A) and $C_7H_7D_2N$ (B).

a technique unique in combining both microscopic time- and length-scale resolution. Moreover, neutrons are scattered by the nuclei, greatly simplifying the modeling of the collected data. Because of these characteristics, this technique is very valuable for an understanding of the molecular origins of different dynamical processes. For example, at least two dynamical processes have already been reported for *m*-toluidine using light scattering and dielectric relaxation measurements.[6,16] However, to the best of our knowledge, the temperature dependence of the relaxational dynamics of the system was not accurately studied as a function of temperature using neutron scattering techniques. Moreover, only a preliminary set of data has been shown for a wavevector transfer value $Q = 0.5$ Å$^{-1}$, corresponding to the prepeak.[17]

In the present work, we studied the dynamics of *m*-toluidine in the liquid and supercooled states. In particular, taking advantage of the spatial resolution of the QENS technique, we measured the characteristic relaxation time of the scattering length density fluctuations, at $Q = 0.5$ Å$^{-1}$, over the length scale characteristic of the intercluster distance, 12 Å. In this way, using partially deuterated samples, it was possible to directly investigate the dynamical behavior of the clusters on approaching the glass transition. This dynamics was compared to the relaxational processes measured at other $Q$ values in the range from ≈0.8 Å$^{-1}$ to ≈2.2 Å$^{-1}$. Two instruments were employed for this study, namely a time-of-flight (ToF) and a neutron spin echo (NSE) spectrometer. The former allowed the investigation of the relaxational dynamics over length scales ranging from ≈8 Å to ≈3 Å in the time range from ≈1 ps to ≈100 ps. The latter was employed to investigate the dynamics up to 15 ns at specific length scales relevant for this study, in particular the interparticle and the intercluster distances.

Section II describes the experimental details of the study. Section III reports the obtained results together with a discussion of their relevance for a better understanding of *m*-toluidine's relaxation dynamics at a molecular level. Section IV is devoted to our conclusions.

## II. EXPERIMENTAL DETAILS

### A. Samples

Four *m*-toluidine samples, differing in isotopic composition, were employed in the study. A perdeuterated sample ($CD_3$–$C_6D_4$–$ND_2$) was purchased from C/D/N Isotopes.[18] A fully hydrogenated ($CH_3$–$C_6H_4$–$NH_2$) sample was purchased from Sigma-Aldrich.[18] For both these samples, the liquid, transparent with slight yellow coloration, was used without further purification. Two partially deuterated samples were prepared at the Center for Nanophase Materials Sciences at the Oak Ridge National Laboratory (ORNL). Selectively deuterated m-toluidines were synthesized using a catalyzed H-D exchange reaction as outlined in the scheme reported in Fig. 1.[19] In a typical experimental procedure, *m*-toluidine (14.6 g, 0.136 mol, Aldrich,[18] 99%), 10% Pd/C (1.48 g, Aldrich,[18] 10 wt. % of substrate), and 5% Pt/C (2.83 g, Aldrich,[18] 20 wt. % of substrate) in $D_2O$ (486 g, Cambridge Isotope Laboratories,[18] 99%) were charged into a 1.2 l stainless steel Parr reactor.[18] After purging with nitrogen for 30 min and hydrogen for 5 min, the reactor was heated to 180 °C while stirring and kept at that temperature for 32 h. After cooling to room temperature, the mixture was diluted with ethyl acetate (EtOAc) (240 ml), and then filtered. The filtrate was washed with EtOAc (3 × 50 ml). The combined organic layers were washed with 50 ml deionized $H_2O$ (for partially deuterated $C_7H_2D_7N$, compound A in Fig. 1) and dried over anhydrous $MgSO_4$. After removing the solvent under vacuum, the desired product was obtained through high vacuum short-path distillation over calcium hydride ($CaH_2$). The amount of partially deuterated $C_7H_2D_7N$ was 9.22 g (started with 14.6 g of *m*-toluidine; isolated yield: 59.3%). The other partially deuterated $C_7H_7D_2N$ sample (compound B in Fig. 1) was obtained by simple H/D exchange in $D_2O$. In a typical procedure, 16.5 g of *m*-toluidine (0.154 mol) was mixed with ≈25 g of $D_2O$ in a 100 ml separatory funnel. After shaking at least 3 times, the aqueous layer was removed. The same procedure was repeated two more times with fresh $D_2O$. The partially deuterated *m*-toluidine-$d_2$ was also further purified by short-path high vacuum distillation over $CaH_2$. The total amount collected was ≈13.1 g (78% recovery). The products were colorless oily liquids and were characterized with gas chromatography mass spectroscopy and nuclear magnetic resonance.

Most of the results reported in this paper were obtained using the perdeuterated sample in which the incoherent signal can be neglected, as shown in the following. However, it is well known[8] that the prepeak is more evident in a partially deuterated sample; on the other hand, in such samples the incoherent signal is not negligible and therefore the separation of the coherent and incoherent contributions is not trivial. Therefore, partially deuterated samples and a hydrogenated sample were only used for a set of measurements aimed at the specific investigation of the cluster dynamics,

using a technique to eliminate the incoherent signal, as will be explained in more detail in Sec. III B. The samples were put in aluminum sample containers and were arranged in an annular geometry with ≈1 mm thickness for the $C_7D_9N$ and $C_7H_2D_7N$ samples and ≈0.15 mm thickness for the $C_7H_7D_2N$ and $C_7H_9N$ samples. During the measurements the samples were placed in a closed cycle refrigerator which allowed control of temperature with an accuracy better than 0.1 K.

### B. Quasielastic neutron scattering measurements: Time-of-flight

In a quasielastic neutron scattering measurement on a traditional (as opposed to a spin echo) spectrometer,[20] the experimentally measured quantity is the double differential scattering cross section, $\frac{\partial^2\sigma}{\partial\mathbf{\Omega}\partial E}$, defined as the probability that a neutron is scattered in the solid angle comprised between $\mathbf{\Omega}$ and $\mathbf{\Omega} + d\mathbf{\Omega}$, exchanging an energy with the sample comprised between $E$ and $E + dE$. In a ToF instrument, the energy exchanged by the neutron with the sample is measured by determining the time that each detected neutron takes to travel from the sample to the detector. The double differential scattering cross section is proportional to the dynamic structure factor as measured by neutrons, $S^n_{ToF}(\mathbf{Q}, E)$,

$$\frac{\partial^2\sigma}{\partial\mathbf{\Omega}\partial E} = \frac{\mathbf{k}_f}{\mathbf{k}_i} S^n_{ToF}(\mathbf{Q}, E),$$

where $\mathbf{k_i}$ and $\mathbf{k_f}$ are the incoming and scattered neutron wavevectors, respectively, and the wavevector transfer is defined as $\mathbf{Q} = \mathbf{k}_i - \mathbf{k}_f$. The exchanged energy $E$ is defined as $E = E_i - E_f$, $E_i$ and $E_f$ being the initial and final energy of the neutron, respectively.

$S^n_{ToF}(\mathbf{Q}, E)$ is the sum of the coherent, $S^n_{coh}(\mathbf{Q}, E)$, and incoherent, $S^n_{inc}(\mathbf{Q}, E)$, neutron dynamic structure factors

$$S^n_{ToF}(\mathbf{Q}, E) = S^n_{coh}(\mathbf{Q}, E) + S^n_{inc}(\mathbf{Q}, E).$$

In a sample with $n$ different types of atoms, the neutron coherent dynamic structure factor can be defined as the sum of the dynamic structure factors of all pairs of atomic species $\alpha$ and $\beta$,

$$S^n_{coh}(\mathbf{Q}, E) = \frac{1}{N}\sum_{\alpha=1}^{n}\sum_{\beta=1}^{n} b^{coh}_\alpha b^{coh}_\beta \sqrt{N_\alpha N_\beta} S^{\alpha\beta}(\mathbf{Q}, E),$$

where $N$ is the total number of atoms, $b^{coh}_\alpha$ is the coherent scattering length of the $\alpha$ atoms, and

$$S^{\alpha\beta}(\mathbf{Q}, E) = \frac{1}{2\pi\sqrt{N_\alpha N_\beta}}\sum_{i_\alpha=1}^{N_\alpha}\sum_{i_\beta=1}^{N_\beta} \times \int_{-\infty}^{\infty}\langle e^{\{i[\mathbf{Q}\cdot\mathbf{R}_{i_\alpha}(t)-\mathbf{Q}\cdot\mathbf{R}_{i_\beta}(0)]\}}\rangle e^{(-iEt)}dt,$$

$N_\alpha$ being the number of atoms of the $\alpha$ species in the sample.

The neutron coherent dynamic structure factor is the Fourier transform of the neutron coherent intermediate scattering function (ISF), defined as

$$I^n_{coh}(\mathbf{Q}, t) = \frac{1}{N}\sum_{\alpha=1}^{n}\sum_{\beta=1}^{n} b^{coh}_\alpha b^{coh}_\beta \sqrt{N_\alpha N_\beta} I^{\alpha\beta}(\mathbf{Q}, t),$$

where

$$I^{\alpha\beta}(\mathbf{Q}, t) = \frac{1}{\sqrt{N_\alpha N_\beta}}\sum_{i_\alpha=1}^{N_\alpha}\sum_{i_\beta=1}^{N_\beta}\langle e^{\{i[\mathbf{Q}\cdot\mathbf{R}_{i_\alpha}(t)-\mathbf{Q}\cdot\mathbf{R}_{i_\beta}(0)]\}}\rangle.$$

As far as the incoherent contribution is concerned, in hydrogenated samples, because the incoherent scattering length of hydrogen is much larger than that of any other isotope, its contribution often approximates to that of the hydrogen atoms only. Thus, the incoherent dynamic structure factor can be easily defined in terms of the self-dynamics of the hydrogen atoms only,

$$S^n_{inc}(\mathbf{Q}, E) = \frac{1}{N} b^{inc}_H S^H_{inc}(\mathbf{Q}, E),$$

where $b^{inc}_H$ is the hydrogen incoherent scattering length and

$$S^H_{inc}(\mathbf{Q}, E) = \frac{1}{2\pi N_H}\sum_{i=1}^{N_H}\int_{-\infty}^{\infty}\langle e^{\{i[\mathbf{Q}\cdot\mathbf{R}_{i_H}(t)-\mathbf{Q}\cdot\mathbf{R}_{i_H}(0)]\}}\rangle e^{(-iEt)}dt,$$

where $\mathbf{R}_{i_H}$ is the position of the i-th hydrogen atom.

The corresponding ISF is defined as

$$I^H_{inc}(\mathbf{Q}, t) = \frac{1}{N_H}\sum_{i=1}^{N_H}\langle e^{\{i[\mathbf{Q}\cdot\mathbf{R}_{i_H}(t)-\mathbf{Q}\cdot\mathbf{R}_{i_H}(0)]\}}\rangle,$$

with $S^H_{inc}(\mathbf{Q}, E) = FT\{I^H_{inc}(\mathbf{Q}, t)\}$, where $FT\{\}$ indicates the Fourier transform operation.

In an amorphous sample, $\mathbf{Q}$ becomes a scalar variable, $Q$.

The ToF measurements were performed on the disk chopper spectrometer (DCS) at the NIST Center for Neutron Research (NCNR).[21] The incoming neutron wavelength was 5 Å and the spectrometer was operated in the "low resolution" mode. In this condition, the experimental resolution function has a full width at half maximum of ≈100 $\mu$eV. Data were collected from 220 K to 300 K in 20 K steps. An additional measurement at 20 K, where all the relaxation dynamics of the system is frozen in the time window of the instrument, was used as a resolution function. A measurement performed on a vanadium standard was used for detector normalization. Using the package MSLICE of the software DAVE,[22] the data were reduced to dynamical structure factor spectra, $S(Q, E)$, at 15 fixed wavevector transfers, $Q$, where

$$Q = \sqrt{\frac{2m_n}{\hbar}[2E_i - E - 2\cos\theta\sqrt{E_i(E_i - E)}]}, \quad (1)$$

$m_n$ and $\theta$ being the neutron mass and the scattering angle, respectively. The obtained spectra were Fourier transformed to the time domain and the instrumental resolution function was deconvolved using the package available in DAVE.[22]

### C. Quasielastic neutron scattering measurements: Neutron spin echo

NSE spectrometers use the Larmor precession of the neutrons' magnetic moment of an incoming polarized beam in the magnetic field of two large solenoids, one placed before and one placed after the sample, as an internal clock, thus measuring the energy exchanged between the scattered neutron and the sample. The experimentally determined

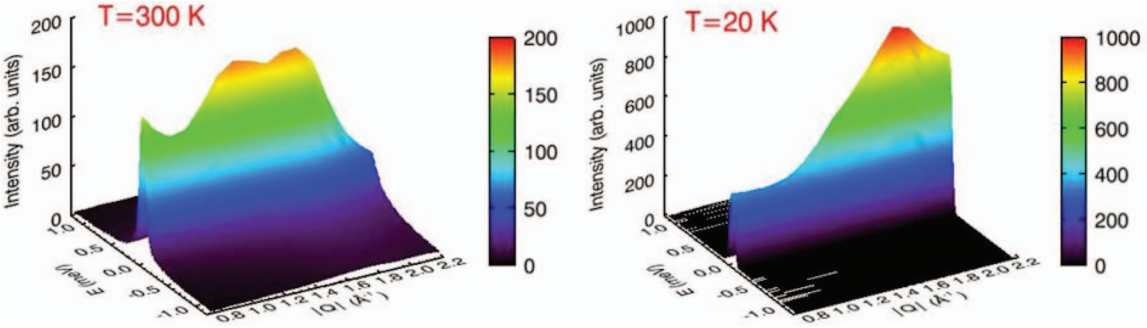


FIG. 2. The dynamic structure factor for deuterated *m*-toluidine at T = 300 K and T = 20 K, as measured on DCS. Note that in the two plots the vertical axis scales are different. Also the slight upturn in the peak intensity in the T = 300 K data at low $Q$, is not related to the prepeak but is due to the sharpening of the QENS spectra because of the slowing down of the dynamics at low-$Q$.

quantity is the number of neutrons transmitted through a neutron polarization analyzer. The amplitude, $A^{echo}$, of the echo signal, as the difference in the field integrals[23] of the first and second arms is varied, is proportional to $I(Q, t_F)$. The value of the time, often referred in this context as Fourier time, $t_F$, is determined by the value of the field integral. The amplitude of the echo for $t_F = 0$, equal to the static structure factor, $I(Q, 0) = \int_{-\infty}^{\infty} S(Q, E)dE = S(Q)$, can be measured by setting up the instrument in such a way that the neutrons magnetic moments and solenoid magnetic field are aligned, thus zeroing the Larmor precession. Two values are measured, usually defined as *Up* and *Dwn*, the number of neutrons reaching the detector through the analyzer with the incoming beam polarization unchanged and reversed, respectively. The normalized ISF is thus obtained as[24–27]

$$\frac{I^n_{NSE}(Q,t)}{I^n_{NSE}(Q,0)} = \frac{2A_{echo}}{Up - Dwn}. \quad (2)$$

It should be kept in mind that, since the incoherent scattering process has a 2/3 probability of flipping the neutron's spin direction,

$$I^n_{NSE}(Q,t) = I^n_{coh}(\mathbf{Q},t) - \frac{1}{3}I^n_{inc}(\mathbf{Q},t).$$

For simplicity, in the remainder of the paper the superscript $n$ as well as the subscripts *ToF* and *NSE* will be omitted, since the origin of the data will be clearly specified in the text.

Most of the NSE measurements were performed on the neutron spin echo spectrometer at the NCNR.[24] The incoming neutron wavelength, λ, was 6 Å with a $\Delta\lambda/\lambda \approx 17.5\%$, which allowed the investigation of the time range from 7 ps to 15 ns. Data were collected (i) at $Q = 0.5$ Å$^{-1}$, corresponding to the prepeak, (ii) at $Q = 1.3$ Å$^{-1}$, corresponding to the molecular CC distance,[9] and (iii) at $Q = 1.7$ Å$^{-1}$, the maximum of the structure factor peak in the fully deuterated sample. A measurement at 10 K was used to determine experimentally the resolution function. Data were reduced to the normalized intermediate scattering function, $I(Q, t)/I(Q, 0)$, using routines available in DAVE.[22]

Additional NSE measurements were performed at the NSE instrument at the spallation neutron source (SNS) at the ORNL.[28,29] The measurements were done with a wavelength band from 4.94 Å to 7.96 Å, respectively, in 42 time channels. Just one given scattering angle was taken to finally reveal momentum transfers between 0.39 Å$^{-1}$ and 0.64 Å$^{-1}$ of the 30 cm × 30 cm detector. Due to the rather low scattering intensity of the sample integration over all time channels was performed. This is equivalent to the use of an effective average incoming neutron wavelength of 6.5 Å. In this configuration the obtained Fourier time span a range from 5 ps and 30 ns. The average $Q$ value was finally ≈0.5 Å$^{-1}$.

## III. RESULTS AND DISCUSSION

Figure 2 reports the dynamic structure factor of *m*-toluidine measured by DCS at T = 300 K and T = 20 K. At T = 300 K, the main diffraction peak is bimodal with a feature centered at ≈1.3 Å$^{-1}$ and one centered at ≈1.7 Å$^{-1}$. In diffraction experiments on the same sample such bimodal character is not evident[9] and the peak at ≈1.3 Å$^{-1}$ is only a shoulder much like in the T = 20 K case. However, it is known that the peak (or shoulder) at ≈1.3 Å$^{-1}$ is related to the aromatic rings center-to-center distance.[9] In fact, in a partially deuterated sample the maximum of the main diffraction peak is shifted closer to this $Q$ value.[8] The most visible feature from Fig. 2 is the $Q$ dependence of the height of the quasielastic peak which is the elastic structure factor, $S(Q, E \approx 0)$, measured within the elastic channel resolution of the spectrometer. Therefore, the finding reported in Fig. 2, which highlights the difference between the elastic, $S(Q, E \approx 0)$, and the static structure factor, $S(Q)$, is not totally surprising but is remarkable in that it clearly shows that the dynamics at the length scales corresponding to the two maxima are distinct. At T = 300 K, a quasielastic broadening is clearly evident, whereas at T = 20 K the elastic peak width is determined by the instrumental resolution function.

### A. NSE results on perdeuterated *m*-toluidine

Figure 3 shows the structure factor of the perdeuterated sample as measured on the NIST NSE spectrometer. Although the instrument is not optimized for static measurements, using polarized neutrons allows to separate the coherent and incoherent scattering contributions. This is easily obtained by the measurement of both non-spin flipped and spin-flipped scattered neutrons, because only the incoherent scattering contributes to the spin-flip scattering with a weighting factor of

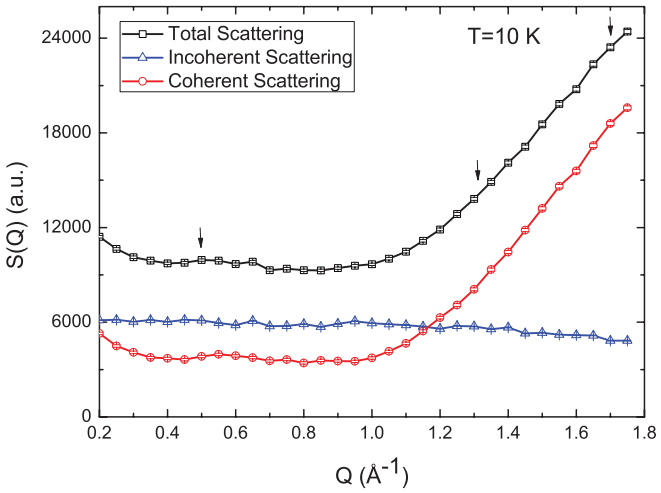


FIG. 3. The structure factor for perdeuterated *m*-toluidine at T = 10 K as measured on NSE. Using polarized neutrons it was possible to separate the coherent and incoherent scattering contributions. Note that the contribution from the empty can (negligible except at small $Q$) was not subtracted. The arrows mark the $Q$ values where NSE measurements were performed. Here and throughout the paper error bars represent one standard deviation.

2/3. The data are in agreement with previous results, although the prepeak is hardly visible, probably because of the poor $Q$ resolution of the instrument. Although it has been reported that the main diffraction peak changes with temperature,[9] no significant temperature dependence of $S(Q)$ was evident in the investigated temperature range within the accuracy of the measurements performed. Note that as far as the dynamic NSE experiment is concerned, the incoherent contribution to the measured echo is weighted by the factor −1/3. The arrows in the plot indicate the $Q$ values where NSE measurements were performed.

Figure 4 reports the normalized dynamic structure factor, $I(Q, t)/I(Q, 0)$, measured by NSE at $Q = 0.5$ Å$^{-1}$, $Q = 1.3$ Å$^{-1}$, and $Q$=1.7 Å$^{-1}$ in plots (a), (b) and (c), respectively. Only one relaxation process appears in the investigated time window. We do not observe any sign of additional incoherent dynamics, which would show up as a negative relaxation component, as all the collected data points are positive within experimental uncertainties. For $Q$ values higher than ≈1.2 Å$^{-1}$ this is easily explained considering that the coherent scattering is ≈4 or more times larger than the incoherent contribution. However, at $Q = 0.5$ Å$^{-1}$ the incoherent contribution amounts to slightly less than $\frac{1}{2}$ of the coherent one. In this case, the lack of any incoherent dynamics signature could be explained, for example, by the fact that such dynamics is outside the experimental window. Another possibility is that coherent and incoherent dynamics have similar relaxation times. In this case the effect of the presence of the incoherent contribution would only reduce the value of $I(Q, t)/I(Q, 0)$ at the lowest time values investigated. As will be discussed in more detail in Sec. III B, this latter possibility seems to be the most likely based on additional measurements which will be discussed next. In general, however, the fact that $I(Q, t)/I(Q, 0)$ does not extrapolate to 1 at $t = 0$ indicates that at least one additional fast relaxation process is present in the system, although too fast to be measured on NSE. It is

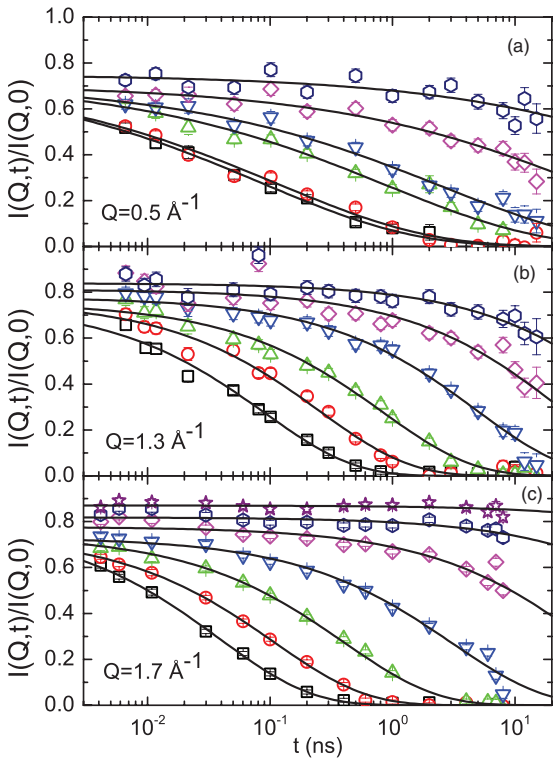


FIG. 4. Plot (a), (b), and (c) show the normalized dynamic structure factor of deuterated *m*-toluidine measured by NSE at Q = 0.5 Å$^{-1}$, Q = 1.3 Å$^{-1}$, and Q = 1.7 Å$^{-1}$, respectively. Squares: T = 260 K; circles: T = 250 K; up triangles: T = 240 K; down triangles: T = 230 K; diamonds: T = 220 K; hexagons: T = 210 K; stars: T = 200 K.

worth mentioning that the data decay to 0, confirming that the longest relaxation time of the system is investigated, namely, the $\alpha$-relaxation. The $I(Q, t)/I(Q, 0)$ curves were analyzed in terms of a stretched exponential decay,

$$\frac{I(Q,t)}{I(Q,0)} = A \exp\left[-\left(\frac{t}{\tau}\right)^{\beta}\right]. \quad (3)$$

As can be seen in Fig. 5 plot (a) the fitting results for the stretched exponent values are temperature independent within the experimental uncertainties in the temperature range from T = 220 K to T = 260 K (a temperature interval where the $\beta$ values can be obtained more reliably as the $I(Q, t)/I(Q, 0)$ curves decay mostly within the time range probed by NSE). Therefore, temperature averaged values for $\beta$ could be extracted and used for subsequent analysis of the NSE data. Previous dielectric and mechanical relaxation investigations of the dynamics of *m*-toluidine have reported a $\beta$ value decreasing with temperature.[12,14] However, a more recent investigation of the shear modulus, $G(t)$, of the system in the supercooled state close to the glass transition showed that the time-temperature superposition principle applies,[13] which suggests that $\beta$ could be considered constant as a function of temperature, within a certain accuracy at least in a limited range. The continuous lines in Fig. 4 show the results of the fits with the $\beta$ parameter fixed to the temperature averaged value. The quality of the fits is excellent. Although $\beta$ is temperature independent, it varies significantly with $Q$. From the NSE results, the temperature averaged value of $\beta$ for $Q = 1.3$ Å$^{-1}$

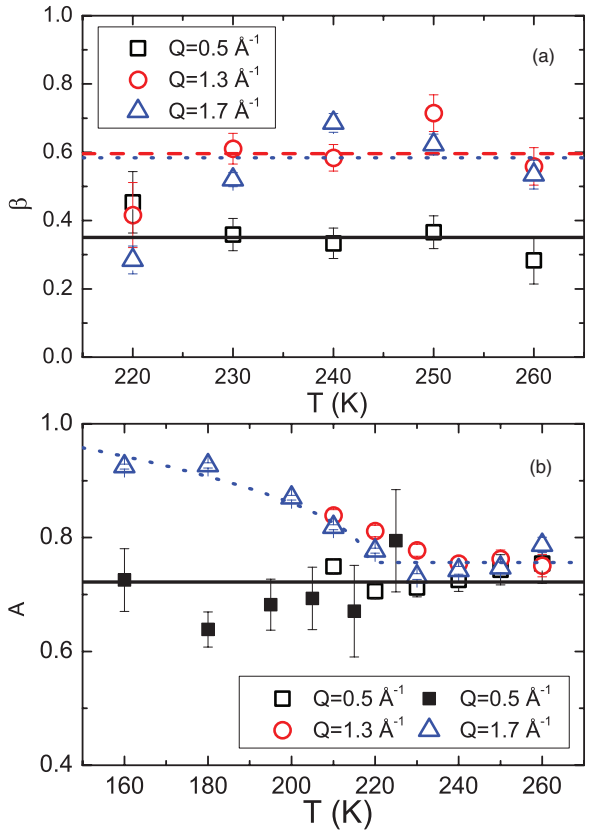


FIG. 5. The results of the fits of the NSE data using a stretched exponential function, Eq. (3). Plot (a) reports the value of $\beta$ which does not show any significant temperature dependence. The horizontal lines represent the temperature averaged values at the three $Q$ values investigated. Plot (b) shows the values obtained for the parameter $A$ after fitting the results with the stretching exponent fixed to its temperature averaged value. Open symbols refer to the data collected on the NCNR NSE whereas the closed black squares are the results of the analysis of the SNS NSE data. The blue dashed line is the fit of the $Q = 1.7$ Å$^{-1}$ data to Eq. (4). The continuous black line is the average value for the $Q = 0.5$ Å$^{-1}$ data.

is 0.59 ± 0.01 and for $Q = 1.7$ Å$^{-1}$ it is 0.58 ± 0.01, almost double the value for $Q = 0.5$ Å$^{-1}$, 0.35 ± 0.02. This may originate from a distribution of cluster sizes affecting the relaxation time of the intercluster correlation. However, the results reported in Sec. III B point to a slightly more complex scenario where *m*-toluidine molecules both involved and not involved in the clustering phenomenon determine the relaxation dynamics observed in the perdeuterated samples, even at $Q$ values corresponding to the intercluster distance, introducing a significant heterogeneity of the observed dynamics. Previous mechanical relaxation measurements have shown that close to the glass transition $G(t)$ can be analyzed in terms of a stretched exponential decay with a stretching parameter equal to 0.56.[13] This value is in good agreement with the average stretching exponent value found in the NSE data analysis for $Q = 1.3$ Å$^{-1}$ and $Q = 1.7$ Å$^{-1}$. This finding suggests that the mechanical relaxation is coupled to the dynamics of the molecular centers. On the other hand, the value of $\beta$ close to the glass transition determined from dielectric relaxation measurements by fitting the $\alpha$ peak data to a Cole-Davidson equation is 0.45,[16] intermediate between the values obtained by NSE at the prepeak and at the two $Q$ values investigated near the first structure factor peak. The same set of dielectric data[16] analyzed in terms of a Havriliak-Negami function give values of the shape parameters mapping to[30,31] a $\beta$ of 0.52, closer to the values obtained in this work at $Q$ values close to the structure factor peak.

Figure 5(b) reports the values of the amplitude of the observed $\alpha$-relaxation as a function of temperature, from a fit of the intermediate scattering function using Eq. (3) and fixing the stretching exponent to its temperature averaged value. According to MCT the amplitude of the $\alpha$-relaxation is constant and equal to the critical non-ergodicity parameter, $f_Q^c$, above the kinetic glass transition temperature, $T_c$. $T_c$ is defined as the temperature at which the density correlator, in this case coinciding with $I(Q, t)/I(Q, 0)$, diverges, not decaying within the experimental time window, taking a constant value equal to $f_Q^c$. It has been suggested that for *m*-toluidine $T_c \approx 228$ K,[7] although values as high as 233 K and as low as 220 K have been obtained as well from a different analysis.[6] Below $T_c$ the amplitude should follow a square-root temperature behavior

$$A = f_Q^c + h_Q\sqrt{\frac{T_c - T}{T_c}}. \tag{4}$$

From Fig. 5(b) it can be seen that for $Q = 1.3$ Å$^{-1}$ and $Q = 1.7$ Å$^{-1}$ the obtained values of $A$ obey the prediction of MCT. In particular, for $Q = 1.7$ Å$^{-1}$, the $A$ values were fitted to Eq. (4) obtaining the following results: $f_Q^c = 0.756 \pm 0.003$, $h_Q = 0.36 \pm 0.01$, and $T_c = 218.2$ K ± 1.3 K. The obtained result for $T_c$ is within the range of values suggested in previous studies.[6,7] It should be noted that $f_Q^c + h_Q$ is greater than one, which is not physically sound. The probable cause of this result is an inaccuracy in the estimation of $h_Q$ which is obtained in a too limited range of temperature insufficiently distant from $T_c$ for an accurate fitting. We conclude that the error in the determination of $h_Q$ is greater than 30%.

The value obtained for the non-ergodicity parameter as reported from inelastic x ray scattering (IXS) measurements[7] is in agreement with the present results. On the other hand, the value of $f_Q$ obtained from light scattering measurements[6] is much lower. Such a discrepancy can be explained by the fact that the two measurements are taken at very different $Q$ values. In fact, the values obtained from IXS for $f_Q$ at $Q$ values smaller than 0.4 Å$^{-1}$ show a sharp decrease which could be consistent with an extrapolated value at $Q \to 0$ of $f_Q \approx 0.4$, in agreement with the results obtained by light scattering. The likely origin of this $Q$ dependence is the effect of the structure factor whose profile should be mirrored by $f_Q$. However, it should be pointed out that the non-ergodicity parameter does not always exactly reproduce the structure factor and that the $Q$ behavior of $S(Q)$ in the hydrodynamic limit is not easily obtained experimentally in a neutron diffraction experiment. Notwithstanding these considerations the effect of the structure factor is a reasonable explanation for the difference between the values of $f_Q$ obtained in this work and by IXS with respect to the results obtained by light scattering.

The $A$ values for $Q = 0.5$ Å$^{-1}$ do not show any increase below $T_c$, as was found from the measurements obtained using the SNS NSE for T as low as 140 K. Within experimental uncertainties, the amplitude is independent of temperature

and takes the value $0.72 \pm 0.01$. The previous IXS study[7] did not explicitly report the results for the non-ergodicity parameter corresponding to the cluster peak. However, the data just above and below $Q = 0.5$ Å$^{-1}$ show a similar temperature behavior to what was found here at $Q = 1.7$ Å$^{-1}$, and there was no mention of a particular behavior at $Q \approx 0.5$ Å$^{-1}$. As mentioned above, $A$ values obtained from the fitting of the NSE data at $Q = 0.5$ Å$^{-1}$ could be affected by an incoherent dynamic contribution. However, it is not clear how this would result in a temperature independent value of the non-ergodicity parameter. The increase of the non-ergodicity parameter at $T < T_c$ originates from the freezing of the microscopic dynamics within the cage of the first neighbor shell. With the present results, it can only be speculated that at length scales corresponding to the intercluster distance the temperature dependence of the microscopic dynamics is different from what was observed corresponding to the structure factor peak. The available data are not sufficient to validate a physical picture that is able to explain this finding. However, a possible explanation is that, if the observed dynamics is related to the motion of *m*-toluidine molecules leaving the cluster, the short dynamics of such molecules, before the $\alpha$-relaxation dynamics initiate, is qualitatively different from that of the molecules not involved in the clustering. As will be shown in the following, there is strong evidence that the dynamics corresponding to the cluster peak is dominated by the time scale of the single particle dynamics of the *m*-toluidine molecules leaving the clusters.

When dealing with the stretched exponential function, which indicates the presence of a distribution of relaxation times, it is customary to report the results in terms of the average relaxation time, $\langle\tau\rangle$, defined as the zeroth moment of the stretched exponential function,

$$\langle\tau\rangle = \int_0^\infty dt \exp^{-(t/\tau)^\beta} = \frac{\tau}{\beta}\Gamma\left(\frac{1}{\beta}\right). \quad (5)$$

Average relaxation values, $\langle\tau\rangle$, obtained by fitting the data using Eq. (3) and fixing the stretching exponent to its temperature averaged value, are reported in Fig. 6. The results from the NCNR and SNS NSE spectrometers agree satisfactorily confirming the reproducibility of the experiment. As expected because of its fragility, the behavior is strongly non-Arrhenius. The continuous black line in Fig. 6 shows the behavior of the viscosity,[13] arbitrarily scaled, to allow visual comparison with the obtained relaxation times. The viscosity data were parameterized as in Ref. 13 using a Vogel-Fulcher-Tammann (VFT) law,

$$\eta = \eta_0 \exp\left(\frac{B}{T - T_0}\right), \quad (6)$$

with $T_0 = 176.3$ K and $B = 547$ K. As can be seen, the NSE results align themselves roughly parallel to the black line, suggesting that at all three $Q$ values investigated the dynamics is determined by the viscosity of the system.

In order to validate this point, Fig. 7 shows a scaling plot of the collected data where the horizontal axis is the time divided by the viscosity of the system at the corresponding temperature. A similar scaling of NSE data was performed for the investigation of the glass-forming system $LiCl \cdot 6D_2O$, with

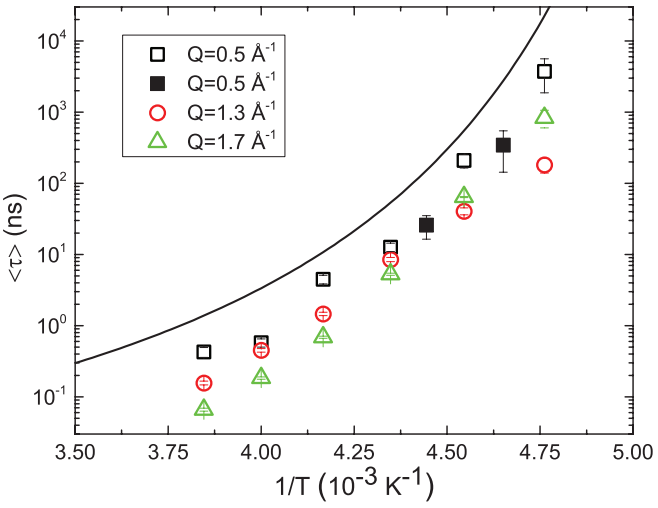


FIG. 6. Arrhenius plot of the average relaxation times $\langle\tau\rangle$ (see Eq. (5)) obtained from the fits of the NSE data using a stretched exponential function, Eq. (3), fixing the stretching exponent to its temperature averaged value. The open symbols refer to the results obtained using the NCNR NSE and the closed squares refers to the results from the SNS NSE. The continuous black line shows the temperature dependence of the viscosity, [13] arbitrarily scaled to allow a comparison to the $\langle\tau\rangle$ values.

the aim of verifying the validity of MCT.[32] However, also because of the presence of a peritectic point in the investigated temperature range, the results were somewhat inconclusive. In the *m*-toluidine case, a previous study has shown that the time-temperature superposition principle applies at 230 K and 256 K, at $Q = 1.3$ Å$^{-1}$ and 2.0 Å$^{-1}$.[17] Here, the data, at $Q$

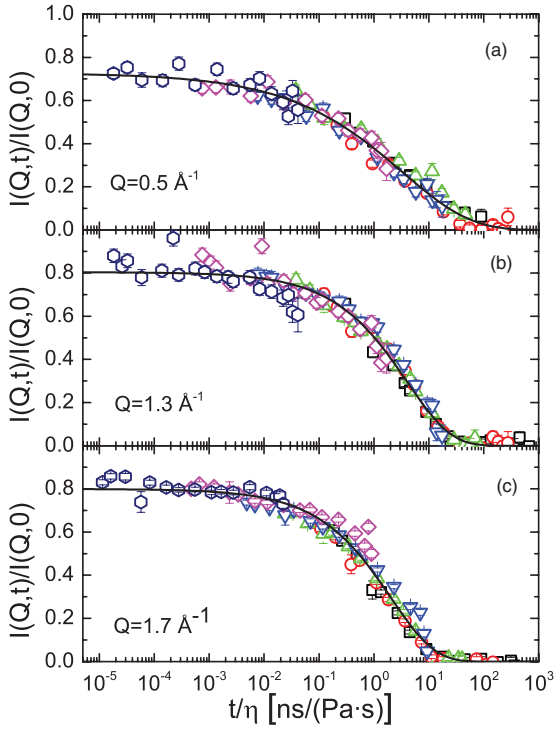


FIG. 7. Plot (a), (b), and (c) show a scaling plot of the normalized dynamic structure factor of perdeuterated *m*-toluidine measured by NSE at Q = 0.5 Å$^{-1}$, Q = 1.3 Å$^{-1}$, and Q = 1.7 Å$^{-1}$, respectively, as a function of the Fourier time divided by the viscosity. [13] Squares: T = 260 K; circles: T = 250 K; up triangles: T = 240 K; down triangles: T = 230 K; diamonds: T = 220 K; hexagons: T = 210 K.

TABLE I. Fitting results for the scaling plot of Fig. 7.

| $Q$ (Å$^{-1}$) | $A$ | $\tau$(T)/$\eta$(T) [.ns/(Pa · s).] | $\beta$ |
|---|---|---|---|
| 0.5 | 0.727 ± 0.010 | 3.33 ± 0.21 | 0.35 ± 0.01 |
| 1.3 | 0.803 ± 0.006 | 4.06 ± 0.10 | 0.54 ± 0.01 |
| 1.7 | 0.799 ± 0.003 | 2.08 ± 0.03 | 0.55 ± 0.01 |

values encompassing the prepeak and structure factor peak ranges, in the temperature range from 260 K to 200 K, nicely fall on the corresponding master curves where the time axis is scaled by the viscosity. A note of caution is in order, since two different VFT regimes have been reported for the relaxation dynamics of *m*-toluidine.[13] However, the crossover between the two regimes has been reported to occur at ≈215 K, at the limit of the temperature range investigated, and therefore it was ignored. It would have been interesting to investigate this crossover but the limitation of the instrumental resolution prevented this study. The good quality of the scaling plots in Fig. 7 indicates that the same relaxation process is responsible for the microscopic relaxation of density fluctuations at the length scales corresponding to both the intercluster and interparticle distances, as well as for the macroscopic flow of the liquid. The scaled data were fitted using a stretched exponential function obtaining the results reported in Table I.

As already anticipated the stretching exponents at $Q$ = 1.3 Å$^{-1}$ and $Q$ = 1.7 Å$^{-1}$ coincide within experimental accuracy, whereas the $\beta$ value for $Q$ = 0.5 Å$^{-1}$ is significantly smaller, which could be rationalized considering that the dynamics probed originates from molecules in a significantly heterogeneous molecular environment. As far as the $A$ values are concerned, again the obtained results at $Q$ = 1.3 Å$^{-1}$ and $Q$ = 1.7 Å$^{-1}$ almost coincide, whereas the value at $Q$ = 0.5 Å$^{-1}$ is slightly smaller. Finally, it is now possible to better appreciate differences in the relaxation times at the different $Q$ values. In fact, the dynamics at $Q$ = 1.7 Å$^{-1}$ is twice as fast as the dynamics at $Q$ = 1.3 Å$^{-1}$. The $Q$ dependence of the dynamics will be discussed in more detail in Sec. III C.

### B. NSE results on partially deuterated m-toluidine samples

By measuring the dynamic structure factor at $Q$ = 0.5 Å$^{-1}$ it was possible to investigate the dynamics of *m*-toluidine at a length scale similar to the intercluster distance. However, it is not certain that the obtained dynamics coincides with that of the clusters themselves. This is because, as shown in Fig. 3 the prepeak as measured on a NSE spectrometer with poor $Q$ resolution is not very evident. Therefore, it is to be expected that different groups of atoms , both involved and not involved in the clustering phenomenon, contribute to the measured $I(Q, t)/I(Q, 0)$. This is confirmed by the finding that the $\beta$ value for $Q$ = 0.5 Å$^{-1}$ is significantly smaller than that measured at $Q$ = 1.3 Å$^{-1}$ and 1.7 Å$^{-1}$.

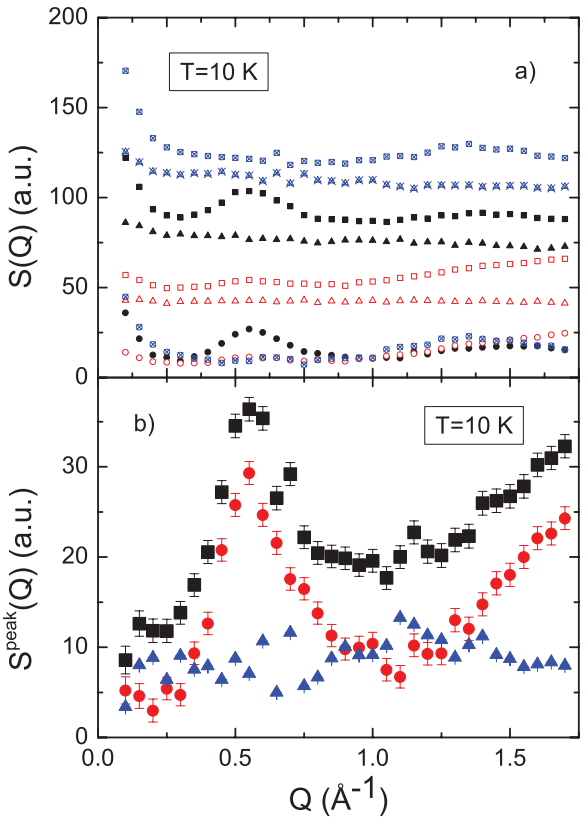


FIG. 8. (a) The structure factor measured by the NCNR NSE spectrometer for $C_7H_7D_2N$ (solid black symbols), for $C_7H_2D_7N$ (open red symbols), and $C_7H_9N$ (starred open blue symbols). Squares, circles, and triangles refer to the total, coherent, and incoherent scattering intensity, respectively. The size of the error bars (not shown) is approximately the same as the size of the symbols. (b) The total (black squares), coherent (red circles), and incoherent (blue triangles) scattering intensity of $S^{peak}(Q)$ as defined in Eqs. (7)–(9), respectively.

In order to address this issue, measurements were performed on two partially deuterated *m*-toluidine samples, namely, $C_7H_2D_7N$ and $C_7H_7D_2N$, and on a fully hydrogenated sample. It is known that the prepeak is more marked in the partially deuterated samples than in a perdeuterated sample. However, in these cases the incoherent contribution is non-negligible which will corrupt any attempt to study the coherent dynamics of the system. In the best case scenario the incoherent dynamics would be observed and in the worst an inextricable mixture of coherent and incoherent dynamics would be measured. This can be seen in Fig. 8 (a) where the structure factors measured on the NCNR NSE for the partially deuterated samples are shown. As expected the prepeak is more evident, especially in the $C_7H_2D_7N$ case, and the incoherent dynamics is dominant.

However, under the assumption that the incoherent scattering of the three samples originates from the hydrogen atoms only, it is possible to eliminate the incoherent contributions and extract the structural feature of the prepeak, by properly combining the measurements of the three samples. The following quantities can be defined

$$S_{coh}^{peak}(Q) = F^{C_7H_2D_7N} S_{coh}^{C_7H_2D_7N}(Q) + F^{C_7H_7D_2N} S_{coh}^{C_7H_7D_2N}(Q) - F^{C_7H_9N} S_{coh}^{C_7H_9N}(Q), \quad (7)$$

$$S_{inc}^{peak}(Q) = F^{C_7H_2D_7N} S_{inc}^{C_7H_2D_7N}(Q) + F^{C_7H_7D_2N} S_{inc}^{C_7H_7D_2N}(Q) - F^{C_7H_9N} S_{inc}^{C_7H_9N}(Q) \approx 0, \quad (8)$$

$$S^{peak}(Q) = S_{coh}^{peak}(Q) + S_{inc}^{peak}(Q) = F^{C_7H_2D_7N} S^{C_7H_2D_7N}(Q) + F^{C_7H_7D_2N} S^{C_7H_7D_2N}(Q) - F^{C_7H_9N} S^{C_7H_9N}(Q) \approx S_{coh}^{peak}(Q), \quad (9)$$

where $F^x = \frac{M_w^x}{M^x T^x}$ and $M_w^x$, $M^x$, and $T^x$ are the molecular weight, mass in the can, and the transmission of the sample $x$, respectively. In Eq. (9), data were corrected for self-shielding and for the number of molecules in the beam, whereas other corrections were neglected, such as the scattering from the sample can, because they are smaller than the statistical error. In particular, multiple scattering effects in the three samples are expected to partly cancel each other and will give a $Q$ independent contribution, unaccounted for in Eq. (9), which is much smaller than the intensity at the prepeak position.

Figure 8(b) shows the result of the above described method. $S^{peak}(Q)$ shows a very intense prepeak with a maximum at $Q \approx 0.6$ Å$^{-1}$ where the incoherent contribution is negligible. Admittedly the procedure is not perfect and affected by significant statistical error but adequate for the objective of minimizing the incoherent contribution.

The idea of Eq. (9) can be applied to obtain the intermediate scattering function of the prepeak at its maximum, $Q = 0.6$ Å$^{-1}$, from Eq. (2)

$$\frac{I^{peak}(Q,t)}{I^{peak}(Q,0)} = \frac{2A_{echo}^{peak}}{Up^{peak} - Dwn^{peak}}, \quad (10)$$

with

$$A_{echo}^{peak} = F^{C_7H_2D_7N} A_{echo}^{C_7H_2D_7N} + F^{C_7H_7D_2N} A_{echo}^{C_7H_7D_2N} - F^{C_7H_9N} A_{echo}^{C_7H_9N}, \quad (11)$$

$$Up^{peak} = F^{C_7H_2D_7N} Up^{C_7H_2D_7N} + F^{C_7H_7D_2N} Up^{C_7H_7D_2N} - F^{C_7H_9N} Up^{C_7H_9N}, \quad (12)$$

$$Dwn^{peak} = F^{C_7H_2D_7N} Dwn^{C_7H_2D_7N} + F^{C_7H_7D_2N} Dwn^{C_7H_7D_2N} - F^{C_7H_9N} Dwn^{C_7H_9N}. \quad (13)$$

It is important to highlight that the summation and subtraction of the three terms have to be performed before calculating the normalized dynamic structure factor.

The rationale behind this procedure is that the coherent dynamics of all the three samples originates from the sum of the dynamic structure factors, $S^{\alpha\beta}(Q, E)$, of the same pairs of atoms, just differently weighted. Therefore, especially at length scales larger than the molecular size, it is expected that combining the coherent dynamic structure factors of the three samples so as to eliminate the incoherent contribution does not alter the information on the dynamics of the system. It would be correct to say that Eqs. (9) and (10) represent a linear combination of scattering cross sections although writing the corresponding equations in terms of the definition of $I_{coh}^n(Q,t)$ will probably not clarify the physical picture. In fact, although it would be possible to explicitly write $S^{peak}(Q)$ in terms of different partial structure factors, $S^{\alpha\beta}(Q, E)$, the target of the present work is to single out the contribution from the clusters of *m*-toluidine molecules rather than to highlight the contribution from particular groups of atoms as is often the case when partially deuterated samples are employed. Concepts used in small angle neutron scattering (SANS) might help explain the underlying idea better. At the length scale corresponding to $Q \approx 0.5$ Å$^{-1}$ a coarse grained approach should still be valid for the present system considering that the cluster size is limited. The use of partially deuterated samples can be thought of as a way to increase the contrast, as defined in SANS, between the clusters and the surrounding molecules, at the expense of an increased incoherent background. Thus, in both partially deuterated samples the structure associated with the clusters is a significant portion of the coherent scattering in the $Q$ range of relevance. Also in the case of the perdeuterated and hydrogenated samples the coherent scattering can be considered, within some approximation,[33] as the sum of the coherent scattering from the clusters with a much smaller contrast and the coherent scattering from the other molecules not involved in the associative behavior. The linear combination of Eqs. (9) and (10) eliminates the incoherent background and the resulting coherent contribution is dominated by the well-contrasted structures related to the clusters. The validity of this approach is verified in retrospect by the fact that $S_{inc}^{peak}(Q,t)$ is almost identically zero and $S_{coh}^{peak}(Q,t)$ shows a clear peak at $Q$ values known to correspond to cluster structures in *m*-toluidine. Therefore, within a certain approximation, $I^{peak}(Q, t)/I^{peak}(Q, 0)$ at $Q = 0.6$ Å$^{-1}$ is assumed to reflect the dynamics of the clusters at the length scale of the intercluster distance. In the perdeuterated sample, where the coherent scattering from the clusters and from all other molecules is of comparable intensity, the scattering length density fluctuations corresponding to the length scale of $\frac{2\pi}{0.5}$ Å$^{-1}$ originating from molecules involved and not involved in clusters is comparable. On the other hand, for the partially deuterated samples those fluctuations originating from the cluster dynamics have a larger contrast and are therefore dominant.

Figure 9 shows the results of the procedure above described for two sets of measurements performed at T = 250 K and 230 K. As can be clearly seen, the dynamics of the prepeak scales with the viscosity. A comparison with the results obtained for the normalized dynamic structure factor of the totally hydrogenated samples shows that it is similar to $I^{C_7H_9N}(Q,t)/I^{C_7H_9N}(Q,0)$. Additional measurements performed on a hydrogenous sample using DCS and the high flux backscattering spectrometer at the NCNR further confirm this finding. This result indicates that the lifetime of the cluster is mainly determined by the single particle dynamics of the individual *m*-toluidine molecules forming the cluster itself. The scaled data need to be fitted using a stretched exponential, Eq. (3), although the $\beta$ exponent is in this case closer to one, indicating that a less heterogeneous dynamics is probed. This finding can be understood considering that in the perdeuterated sample the dynamics of any pair of *m*-toluidine molecules has a roughly equivalent weight in defining the

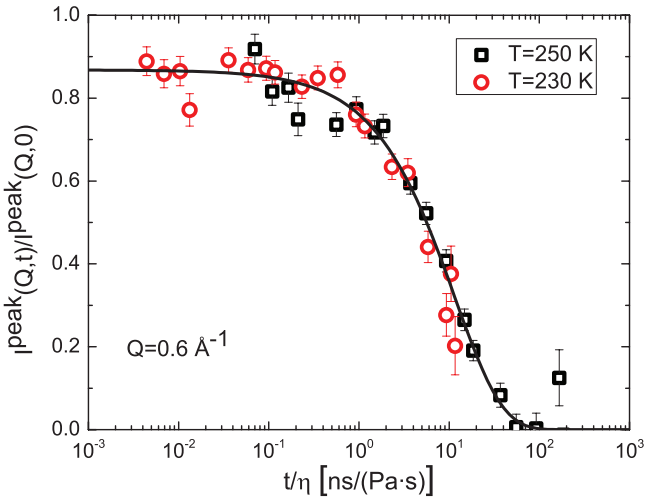


FIG. 9. Scaling plot of the normalized dynamic structure factor $I^{peak}(Q, t)/I^{peak}(Q, 0)$ as defined in Eq. (10), for T = 250 K and 230 K. The continuous line represents the fit of the scaled data to a stretched exponential function, Eq. (3).

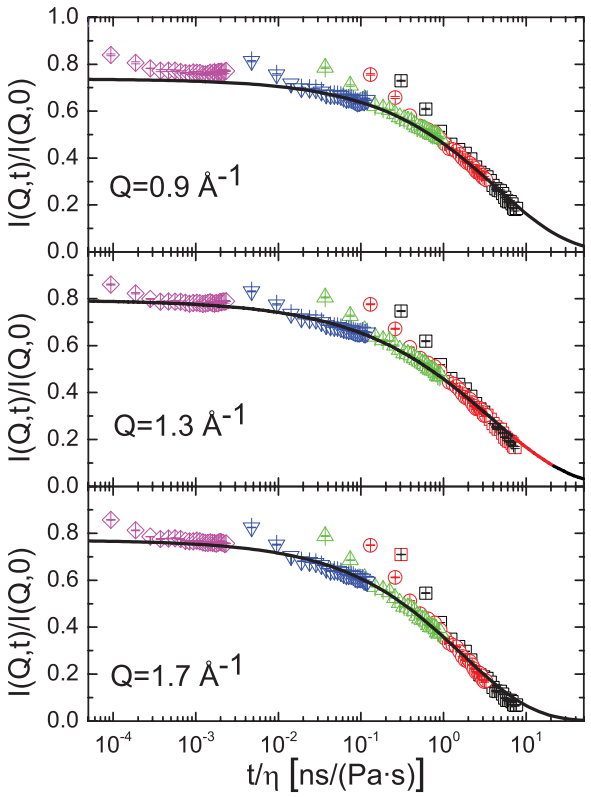


FIG. 10. Scaling plot of the data obtained using the ToF instrument DCS. Squares: T = 300 K; circles: T = 280 K; up triangles: T = 260 K; down triangles: T = 240 K; diamonds: T = 220 K. Continuous lines represent fits to a stretched exponential function, Eq. (3).

coherent intermediate scattering function, irrespective of their microscopic environment, which is probably significantly heterogeneous at supercooled temperatures both structurally and dynamically. The significant stretch of the relaxation function originates from this. By using partially deuterated samples and combining their scattering according to Eqs. (9) and (10), the resulting $I^{peak}(Q, t)/I^{peak}(Q, 0)$ mostly reflects the dynamics of the structures related to the clustering, which have an enhanced scattering contrast, again using a term and concept borrowed from SANS. The fact that the stretching exponent in the case of $I^{peak}(Q, t)/I^{peak}(Q, 0)$ is significantly closer to 1 than in the perdeuterated sample case, indicates that the dynamics of the clusters is significantly less heterogeneous. This could be because each cluster is surrounded by a similar environment as well as because the dynamics of the individual molecules leaving a cluster, thus ending its existence, approximates a simple Debye relaxation process.

### C. ToF results on perdeuterated m-toluidine

In order to investigate in detail the $Q$ dependence of the dynamics of *m*-toluidine, the use of a ToF instrument is more appropriate, because several $Q$ values can be investigated at the same time. On the other hand, the understanding of the temperature dependence of the relaxational dynamics acquired using the NSE spectrometer was used for the analysis of the DCS data. The dynamic structure factor data, Fourier transformed to $I(Q, t)/I(Q, 0)$ curves, were used to obtain viscosity scaled plots of the normalized intermediate structure factor similar to those obtained using NSE. The results for three $Q$ values are shown in Fig. 10, as an example. Note, that in the DCS configuration employed the relaxation times obtained below 0.8 Å$^{-1}$ are not reliable because of the limitation of the resolution function and are not reported. Again the quality of the scaling plot is good confirming the conclusions of Sec. III A of the paper.

In the ToF data, we see a systematic deviation of the data points at short time from scaling behavior. In fact, the short time dynamics which was not in the NSE time window can be appreciated in the DCS data. The investigation of the fast dynamics was carried out in the energy domain. The preliminary results indicate that the fast dynamics has a much smaller temperature dependence than the $\alpha$-relaxation. The time scales involved as well as the temperature dependence of the preliminary results are reminiscent of the behavior obtained from the analysis of polarized and depolarized Brillouin spectra.[6] This would suggest a correlation between the observed fast dynamics and the reorientational dynamics of the *m*-toluidine molecules. However, a more detailed analysis and in depth discussion are necessary before this idea can be validated. These are beyond the scope of the present paper and will be object of a future publication.[34]

The results obtained in this work are summarized in Fig. 11 as a function of $Q$, where the results of the fitting of the scaling plots for both the DCS and NSE data are reported. In general, the agreement between the results obtained using the two spectrometers is remarkable. Plot (a) shows the amplitude $A$, corresponding to the non-ergodicity parameter. According to the MCT, $f_Q^c$ should mirror the behavior of the structure factor. The obtained $A$ values show a broad feature, with values in the range from ≈0.7 to ≈0.8, centered at ≈1.3 Å$^{-1}$ which might reflect the $S(Q)$, although shifted to lower $Q$. As mentioned above, a previous investigation using inelastic x ray scattering[7] has shown a significant reduction of $f_Q^c$ only

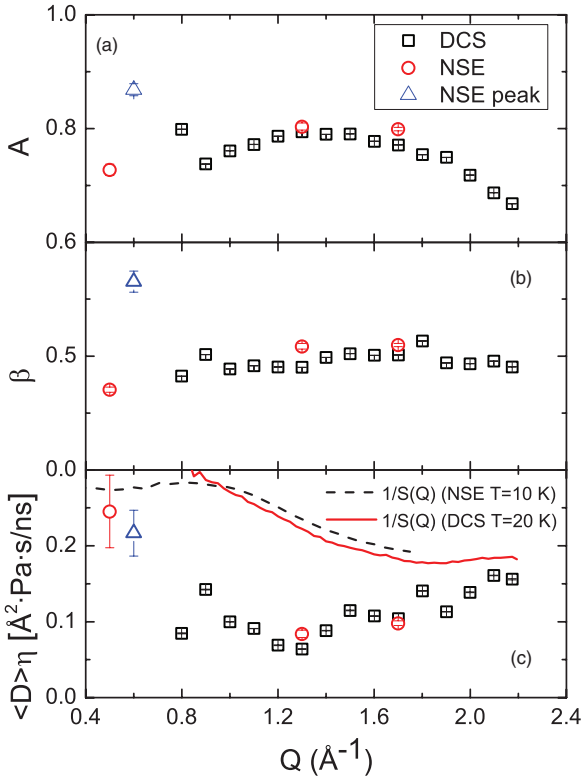


FIG. 11. This figure summarizes the results, as a function of $Q$, of the fitting of the scaled data from both DCS and the NCNR NSE using a stretched exponential function, Eq. (3): (a) the amplitude $A$; (b) the stretching exponent $\beta$, and c) the average diffusion coefficient. In plot (c) the dashed black and continuous red lines represent the inverse of the structure factor as measured on the NCNR NSE (at T = 10 K) and on DCS (at T = 20 K), in an arbitrary scale.

below $Q = 0.4$ Å$^{-1}$. Finally, it is interesting to highlight that $A$ for $I^{peak}(Q, t)/I^{peak}(Q, 0)$ is about 0.9, clearly larger than the value obtained for the perdeuterated sample where, however, as previously explained this value could be affected by the presence of a non-negligible incoherent scattering contribution. As far as the stretching exponent is concerned the values for the perdeuterated sample do not show any significant modulation in $Q$ and are close to 0.5. In the case of the cluster dynamics, as probed through $I^{peak}(Q, t)/I^{peak}(Q, 0)$, $\beta$ is significantly higher indicating that less of a distribution of relaxation times is probed. This has been attributed to the fact that $I^{peak}(Q, t)/I^{peak}(Q, 0)$ is determined mostly by the *m*-toluidine molecules involved in the clustering, a much less diverse ensemble of molecules than those probed, even at the same $Q$ value, in the perdeuterated sample.

On the other hand, it would be more interesting to examine the $Q$ dependence of the diffusion coefficient since evidence of "de Gennes" narrowing has been reported.[17] To do so we define a viscosity corrected quantity proportional to an average diffusion coefficient as

$$\langle D\rangle\eta = \frac{\eta}{\langle\tau\rangle Q^2}, \tag{14}$$

where $\frac{\eta}{\langle\tau\rangle}$ is determined from the fits of the viscosity scaled data.

The obtained results for $\langle D\rangle\eta$ are reported in Fig. 11(c). The inverse of the structure factor in an arbitrary scale, as measured by NSE and on DCS as the integrated intensity of $S(Q, E)$, is shown as well for comparison. A modulation of the average diffusion coefficient can be appreciated. The $Q$ dependence of $\langle D\rangle\eta$ mimics the behavior of $\frac{1}{S(Q)}$, although the slowing down of the dynamics starts at lower $Q$ values than the increase of $S(Q)$. Moreover, the minimum of $\langle D\rangle\eta$ is reached roughly corresponding to the CC length scale rather than at the maximum of $S(Q)$. This finding indicates that the $\alpha$-relaxation probed is related to the motion of the molecule as a whole. It is the first time that "de Gennes" narrowing of the viscosity scaled dynamics in the temperature range encompassing both the liquid and supercooled states is reported for *m*-toluidine.[17] Incidentally, the bimodal behavior of $S(Q, E \approx 0)$ around the structure factor peak position shown in Fig. 2 is not exactly mirrored in the behavior of $\langle D\rangle\eta$. In fact, the viscosity normalized average diffusion coefficient has a minimum at ≈1.3 Å$^{-1}$ followed by a shoulder or slight plateau at higher $Q$. When comparing $\langle D\rangle\eta$ to the height of the quasielastic peak measured on DCS, it should also be considered that the elastic structure factor as seen in Fig. 2 is not normalized by $Q^2$ and depends on $A$ and $S(Q)$. More importantly, the $S(Q, E \approx 0)$ as measured on DCS is affected by the instrumental resolution function. This, depending on the temperature, can significantly affect the relative height of the two contributions at ≈1.3 Å$^{-1}$ and ≈1.7 Å$^{-1}$, especially considering that the $\alpha$ relaxation process is significantly stretched. In fact, where the relaxation rate is smaller, as at ≈1.3 Å$^{-1}$, the height of the quasielastic peak is smeared by the effect of the instrumental resolution more significantly than where the relaxation rate is larger, as at ≈1.7 Å$^{-1}$. A calculation of $S(Q, E \approx 0)$ with an instrumental resolution of ≈100 $\mu$eV starting from the results reported in Fig. 11 yields results consistent with those measured on DCS within the used approximations.[35]

A comparison of the Q dependence of $\langle D\rangle\eta$ and $A$ with respect to $\frac{1}{S(Q)}$ and $S(Q)$ shows that in both cases the behavior of these quantities is offset with respect to the structure factor. Both these findings can be rationalized considering that the shape of $S(Q)$ is strongly affected by the amine and methyl groups' spatial correlation whereas both the diffusive dynamics and the non-ergodicity parameter are related within the MCT to the center-of-mass dynamics. In fact, both $A$ and $\langle D\rangle\eta$ have their extrema, maximum, and minimum respectively, corresponding to the CC distance at ≈1.3 Å$^{-1}$. Taken together these results give strong support to the idea, introduced by the previous NSE study on *m*-toluidine,[17] that the $\alpha$-relaxation dynamics is more directly related to the structure factor corresponding to the center of the molecules rather than to the $S(Q)$ measured not using partially deuterated samples.

No significant slowing down of the diffusion coefficient can be appreciated, however, corresponding to the prepeak, neither for $I^{C_7D_9N}(Q, t)/I^{C_7D_9N}(Q, 0)$ nor for $I^{peak}(Q, t)/I^{peak}(Q, 0)$, indicating that no "de Gennes" narrowing is associated with the prepeak for *m*-toluidine. Moreover, the average diffusion coefficients as measured using the perdeuterated sample and the partially deuterated ones are largely similar, indicating that within a certain approximation, at $Q$ values around 0.5 Å$^{-1}$, the dynamics of the molecules in the clusters is not significantly different, although apparently less heterogeneous, from that of the other *m*-toluidine

molecules. In conclusion, the clusters do not behave dynamically as a whole. Their dynamics coincides with the dynamics of the molecules involved in the formation of the structures. Moreover, the results reported here indicate that the dynamics of these molecules amounts to their single particle dynamics. The picture arising reminds of the one recently suggested for the dynamics of lysozyme molecules in solution, which show a so called "cluster" peak in the SANS spectra but which behave dynamically as independent entities.[36–38]

## IV. CONCLUSION

The dynamics of *m*-toluidine was investigated in the liquid and supercooled states down to the glass transition. Using the QENS technique, and two different types of spectrometers, namely, a ToF and neutron spin echo, the microscopic dynamics at length scales ranging from ≈12 Å to ≈3 Å was investigated. The data show that the microscopic dynamics scales with the macroscopic viscosity in the whole range of temperature and length scale investigated. "de Gennes" narrowing corresponding to the interparticle distance was shown in the temperature range from 300 K to 220 K. Moreover, the dynamics of the system at $Q$ values corresponding to the prepeak, the structure factor feature indicating the distance between *m*-toluidine molecular clusters, was investigated as a function of temperature for the first time. The results obtained using a perdeuterated sample were critically compared with those obtained by combining in a novel method the information contained in the dynamic structure factors of two partially deuterated samples and of the fully hydrogenated sample. Also the obtained dynamics of the clusters scales with the macroscopic viscosity and a comparison with the incoherent dynamics structure factor suggests that the lifetime of the clusters depends on the single particle dynamics of the individual *m*-toluidine molecule in the cluster. The reported results validate the hypothesis by Morineau and Alba-Simionesco[8] that the aggregates correlated to the prepeak are limited in size and do not affect the glass transition phenomenon. It might be interesting to compare this behavior with that of other systems in which the prepeak originates from a stronger and more extensive structuring.

## ACKNOWLEDGMENTS

The authors thank Michihiro Nagao and Madhusudan Tyagi for helpful discussions. This work utilized facilities supported in part by the National Science Foundation under Agreement No. DMR-0944772. This research was partially conducted at the Center for Nanophase Materials Sciences, which is sponsored at Oak Ridge National Laboratory by the Office of Basic Energy Sciences, U.S. Department of Energy.

[1]W. Götze and L. Sjögren, Rep. Prog. Phys. **55**, 241 (1992).
[2]M. T. Cicerone and M. D. Ediger, J. Chem. Phys. **103**, 5684 (1995).
[3]N. T. Correia, C. Alvarez, J. J. M. Ramos, and M. Descamps, J. Chem. Phys. **113**, 3204 (2000).
[4]C. A. Angell, J. Res. Natl. Inst. Stand. Technol. **102**, 171 (1997).
[5]C. A. Angell, J. Non-Cryst. Solids **73**, 1 (1985).
[6]A. Aouadi, C. Dreyfus, M. Massot, R. M. Pick, T. Berger, W. Steffen, A. Patkowski, and C. Alba-Simionesco, J. Chem. Phys. **112**, 9860 (2000).
[7]L. Comez, S. Corezzi, G. Monaco, R. Verbeni, and D. Fioretto, Phys. Rev. Lett. **94**, 155702 (2005).
[8]D. Morineau and C. Alba-Simionesco, J. Chem. Phys. **109**, 8494 (1998).
[9]D. Morineau, C. Alba-Simionesco, M.-C. Bellissent-Funel, and M.-F. Lauthié, Europhys. Lett. **43**, 195 (1998).
[10]R. Chelli, G. Cardini, P. Procacci, R. Righini, and S. Califano, J. Chem. Phys. **116**, 6205 (2002).
[11]R. Chelli, G. Cardini, P. Procacci, R. Righini, and S. Califano, J. Chem. Phys. **119**, 357 (2003).
[12]M. Cutroni and A. Mandanici, J. Chem. Phys. **114**, 7124 (2001).
[13]A. Mandanici, X. Shi, G. B. McKenna, and M. Cutroni, J. Chem. Phys. **122**, 114501 (2005).
[14]M. Cutroni, A. Mandanici, A. Spanoudaki, and R. Pelster, J. Chem. Phys. **114**, 7118 (2001).
[15]L. Carpentier, R. Decressain, and M. Descamps, J. Chem. Phys. **121**, 6470 (2004).
[16]A. Mandanici, M. Cutroni, and R. Richert, J. Chem. Phys. **122**, 084508 (2005).
[17]C. Alba-Simionesco, A. Tölle, D. Morineau, B. Farago, and G. Coddens, e-print arXiv:cond-mat/0103599v1.
[18]Identification of a commercial product does not imply recommendation or endorsement by the National Institute of Standards and Technology, nor does it imply that the product is necessarily the best for the stated purpose.
[19]N. Ito, T. Watahiki, T. Maesawa, T. Maegawa, and H. Sajiki, Synthesis **9**, 1467 (2008).
[20]M. Bée, *Quasielastic Neutron Scattering* (Hilger, Bristol,1988).
[21]J. R. D. Copley and J. C. Cook, Chem. Phys. **292**, 477 (2003).
[22]R. T. Azuah, L. R. Kneller, Y. Qiu, P. L. W. Tregenna-Piggott, C. M. Brown, J. R. D. Copley, and R. M. Dimeo, J. Res. Natl. Inst. Stand. Technol. **114**, 341 (2009).
[23]The field integral is defined as the integral of the magnetic field experienced by the neutron along its flight path: $\int \mathbf{B} \cdot d\mathbf{l}$.
[24]N. Rosov, S. Rathgeber, and M. Monkenbusch, ACS Symp. Ser. **739**, 103 (2000).
[25]M. Monkenbusch, R. Schätzler, and D. Richter, Nucl. Instrum. Methods Phys. Res. A **399**, 301 (1997).
[26]*Neutron Spin Echo*, Lecture Notes in Physics Vol. 128, edited by F. Mezei (Springer-Verlag, Berlin,1980).
[27]*Neutron Spin Echo*, Lecture Notes in Physics Vol. 601, edited by F. Mezei, C. Pappas, and T. Gutberlet (Springer-Verlag, Heidelberg, 2003).
[28]M. Ohl, M. Monkenbusch, D. Richter, C. Pappas, K. Lieutenant, T. Krist, G. Zsigmond, and F. Mezei, Physica B **350**, 147 (2004).
[29]M. Ohl, M. Monkenbusch, T. Kozielewski, B. Laatsch, C. Tiemann, and D. Richter, Physica B **356**, 234 (2005).
[30]It is known that there is no analytical relationship between the stretched exponential, often referred to as the Kohlrausch-Williams-Watts (KWW), and the Havriliak-Negami (HN) relaxation functions. However, a relationship between the shape parameters of the HN function, $\alpha_{HN}$ and $\gamma_{HN}$, and the stretching exponent of the KWW function, $\beta_{KWW}$, has been proposed: $\alpha_{HN}\gamma_{HN} = \beta_{KWW}^{1.23}$. [31]
[31]F. Alvarez, A. Alegría, and J. Colmenero, Phys. Rev. B. **44**, 7306 (1991).
[32]B. Prevel, J. Dupuy-Philon, J. F. Jal, J. F. Legrand, and P. Chieux, J. Phys. Condens. Matter **6**, 1279 (1994).
[33]Cross terms, as well as the fact that the molecules forming the clusters can migrate away to be part of the surrounding medium, are neglected in this simple picture.
[34]A. Faraone, Y. Zhang, M. Tyagi, and J. R. D. Copley, "Incoherent dynamics of meta-toluidine" (unpublished).
[35]Some errors are introduced by completely neglecting the short time dynamics which will still contribute to the height of the quasielastic peak. In the time domain, the elastic instrumental resolution of DCS was for this calculation approximated to a Gaussian function with FWHM of 20 ps.
[36]L. Porcar, P. Falus, W. R. Chen, A. Faraone, E. Fratini, K. Hong, P. Baglioni, and Y. Liu, J. Phys. Chem. Lett. **1**, 126 (2010).
[37]Y. Liu, L. P. J. Chen, W. R. Chen, P. Falus, A. Faraone, E. Fratini, K. Hong, and P. Baglioni, J. Phys. Chem. B **115**, 7238 (2011).
[38]P. Falus, L. Porcar, E. Fratini, W. R. Chen, A. Faraone, K. Hong, P. Baglioni, and Y. Liu, J. Phys. Condens. Matter **24**, 064114 (2012).